Low-temperature magnetic properties of Fe nanograins in an amorphous Fe-Zr-B matrix

J. S. Garitaonandia*
Departamento de Electricidad y Electrónica, Facultad de Ciencias, Universidad del País Vasco/EHU, Apartado 644, E-48080 Bilbao, Spain

P. Gorria
Departamento de Física, Universidad de Oviedo, E-33007 Oviedo, Spain

L. Fernández Barquín
CITIMAC, Facultad de Ciencias, Universidad de Cantabria, E-39005 Santander, Spain

J. M. Barandiarán
Departamento de Electricidad y Electrónica, Facultad de Ciencias, Universidad del País Vasco/EHU, Apartado 644, E-48080 Bilbao, Spain

(Received 11 February 1999; revised manuscript received 21 July 1999)

The low-temperature magnetic behavior of $Fe_{87}Zr_6B_6Cu_1$ metallic glasses has been studied by dc magnetization (5–400 K) and RT Mössbauer spectroscopy after a series of thermal treatments. Precipitation of crystalline Fe nanograins is observed, their size (5–15 nm) and amount (1–19%) being dependent on the annealing temperature. The produced structural arrangement provides a model system in order to study the properties of a collection of high-moment ferromagnetic clusters embedded in a weak ferromagnetic matrix. The splitting between the zero-field-cooling and field-cooling magnetization curves increases as the amount of Fe grains does, up to about 6% of the sample volume, and then decreases. This is interpreted as an effect of exchange coupling between the grains through the surrounding amorphous matrix.

I. INTRODUCTION

The mechanisms driving the peculiar properties of Fe-Zr-based amorphous alloys, displaying re-entrant spin glass (RSG) and Invar behavior,[1–5] are still the object of an intense controversy. In particular, some models deal with the existence of magnetic inhomogeneities leading to a noncollinear state with a net ferromagnetic component, when entering into the RSG state.[6] Alternative points of view have put forward the existence of ''spin clusters'' created by density variations in the amorphous state during the casting of the ribbons.[7] Also, it has been suggested that even in these Fe-rich alloys, the observed magnetic phenomena are reminiscent of superparamagneticlike behavior.[8–10] Some recent studies on Fe-Zr-B glasses have indicated that similar mechanisms are present in these alloys at low boron concentrations.[11–13]

On the other hand, these Fe-Zr-B alloys are used to produce nanocrystalline alloys by heating amorphous material and their characterization has boosted an enormous research activity during the early 1990s, mainly focused on technical applications.[14,15] The nanocrystalline state in these alloys is obtained by a precipitation of α-Fe nanometric grains in a remaining amorphous phase using adequate thermal treatments on the as-quenched amorphous alloys. To improve such a precipitation, a small percentage of Cu (around 1%) is commonly included. The important role of this element in these processes has been extensively discussed in the literature.[16–18]

In addition, these nanocrystalline alloys have also procured an exciting field to study the competition of magnetic interactions between the small precipitated Fe-grains and the roles of the remaining amorphous matrix and the nanocrystal-amorphous interfaces. As a consequence, their varied effects are well known nowadays, as regarding the high-temperature properties (coercivity evolution with temperature, Curie temperature changes of the amorphous phase as increased by the exchange field penetration from the nanocrystals, etc.).[19–25]

However, the low-temperature behavior of the same nanocrystalline samples at early stages of crystallization (i.e., with crystalline fractions below 20%) has not been extensively studied,[26,27] although it can provide a model system for studying the properties of a collection of high moment ferromagnetic nanoclusters embedded in a weak ferromagnetic matrix. This view can help to understand the original picture of clusters used for explaining the Fe-Zr glasses behavior.

The main aim of the present work is to carry out a low-temperature study in $Fe_{87}Zr_6B_6Cu$, through a systematic series of thermal treatments giving rise to precipitation of small amounts of α-Fe nanocrystals, whose structure, size, and distribution have been recently studied[20,28] in the same samples. For this we have performed a comparison of the low-temperature magnetization behavior between the reported alloy in an amorphous state and that of samples in an early stage of nanocrystallization. Moreover, the validity of a recently developed model to explain the amorphous/nanocrystalline interplay of the magnetic interactions has been also studied for the case of the original amorphous clusters.

II. EXPERIMENTAL PROCEDURE AND RESULTS

Ribbons of composition $Fe_{87}Zr_6B_6Cu_1$ were prepared by melt spinning in glassy state. Isothermal treatments (1 h annealing at different temperatures) were performed in these

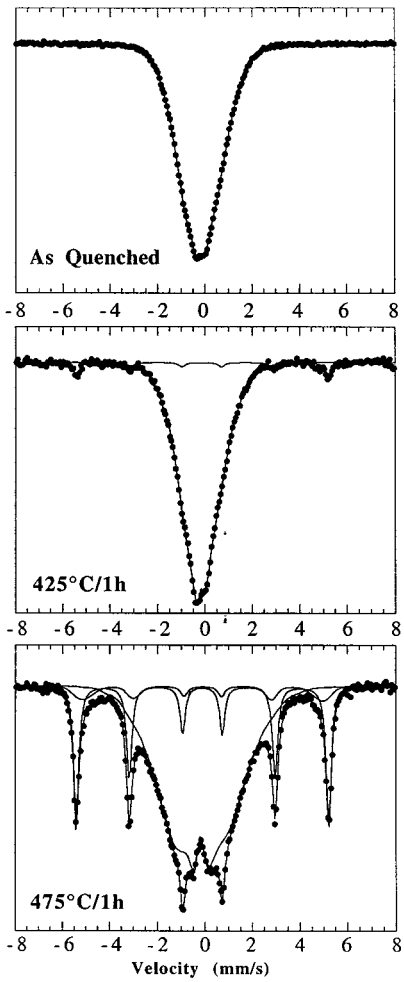

FIG. 1. Mössbauer spectra in selected samples showing the appearance of bcc-Fe nanocrystals after annealing. The sample heated at 475 °C shows also the presence of an ''interface'' with an $B_{HF} = 30$ T.

samples by means of a differential thermal analyzer (DTA) apparatus under flowing Ar atmosphere. The DTA technique provides rapid heating and cooling rates, a continuous monitoring of the temperature and on-line display of any thermal effect occurring during the treatment. X-ray diffraction and Mössbauer spectroscopy were used to characterize the samples microscopically. The results (see, for example, the Mössbauer spectrum of Fig. 1) show a typical amorphous pattern for the as-quenched alloy. The possible existence of minute amounts of very small Fe grains cannot be completely discarded by these techniques, which have a lower detection limit of about 1–2%. In addition, a more sensitive technique to detect eventual small quantities of magnetic grains such as dc magnetization or ferromagnetic resonance (FMR) (Ref. 29) does not show any particular contribution above the Curie temperature of the amorphous phase (see the as-quenched sample in Fig. 2).

After the thermal treatments, the Mössbauer spectra were fitted with a crystalline sextet and a distribution of hyperfine fields, using the NORMOS program developed by Brand, Lauer, and Herlach.[30] In samples treated above 375 °C, the spectra (Fig. 1) show the appearance of Fe crystals as deduced from the sextet with a hyperfine field, $B_{HF} = 33$ T. For the sample treated at 475 °C, the Mössbauer spectrum shows an interesting component with $B_{HF} \approx 30$ T. This has been interpreted as arising from the amorphous-crystal interface,[23,31,32] and extends up to around two atomic layers, as it was demonstrated in Ref. 20. The interface should be also present in samples annealed at other temperatures but the Mössbauer is not sensitive enough to separate that contribution from the amorphous component. The relative amounts of crystal, interface, and amorphous phases have been deduced from the relative areas of the corresponding subspectra, assuming the same recoilless fraction in all cases.

Magnetic measurements shown in Fig. 2 were performed in a superconducting quantum interference device (SQUID) magnetometer between 5 and 400 K. The zero-field-cooling (ZFC) and field-cooling (FC) curves were recorded using $H = 400\ \mathrm{A\,m^{-1}}$, after a careful compensation of stray fields at the sample location. As measurements at higher fields progressively mask the spin-glass behavior as shown in the literature,[2,19] we have limited our measurements to the above-mentioned value. In general terms it is obvious that: (i) Splitting between ZFC and FC curves is present for all the studied samples including the as-quenched one. (ii) FC curves show a flat behavior, due to the demagnetizing factor, and (iii) a sharp decrease at the Curie temperature of the amorphous matrix (less pronounced at the 475 °C stage) is detected. The treatment at 350 °C produces a great amount of structural relaxation and the splitting of the as-quenched sample is reduced. Afterwards it increases as the amount of Fe crystallites does, up to the sample treated at 450 °C, while annealing at 475 °C reduces the splitting effect again. At this temperature the decrease of the magnetization at T_C is broadened and the transition extends above 400 K, spanning at least 100 K.

To end up with the description of dc magnetization results, it is remarkable to note that the shape of the ZFC curve at very low temperature also shows changes as a function of the annealing. The rapid change of slope in the as-quenched state appearing at about 30 K is not visible in the first stage of annealing, but appears again after the 425 °C stage.

The magnetization remaining above the T_C of the amorphous phase can provide an independent check of the amount of crystalline phase present. However, this is only approximate, as the differences in magnetization and anisotropy between the amorphous and crystalline phases and the evolution of these quantities as a function of the annealing can distort the simple picture relating magnetization to phase amount.

III. DISCUSSION

The description of the data of Fig. 2 reveals that the splitting appearing in the as-quenched amorphous sample is also observed in the samples with a low crystallization fraction. This may indicate that the magnetic mechanisms giving rise to the splitting for all the samples can be basically the same and hence we could consider that the structural arrangements related to those mechanisms should be similar in both states (amorphous and nanocrystalline). In the as-quenched (AQ) state, this arrangement has been described by the existence of inhomogeneities of amorphous nature (often referred as clusters in the literature)[2,9] whereas in our nanocrystalline samples at the early stage (hereafter referred as ES), these

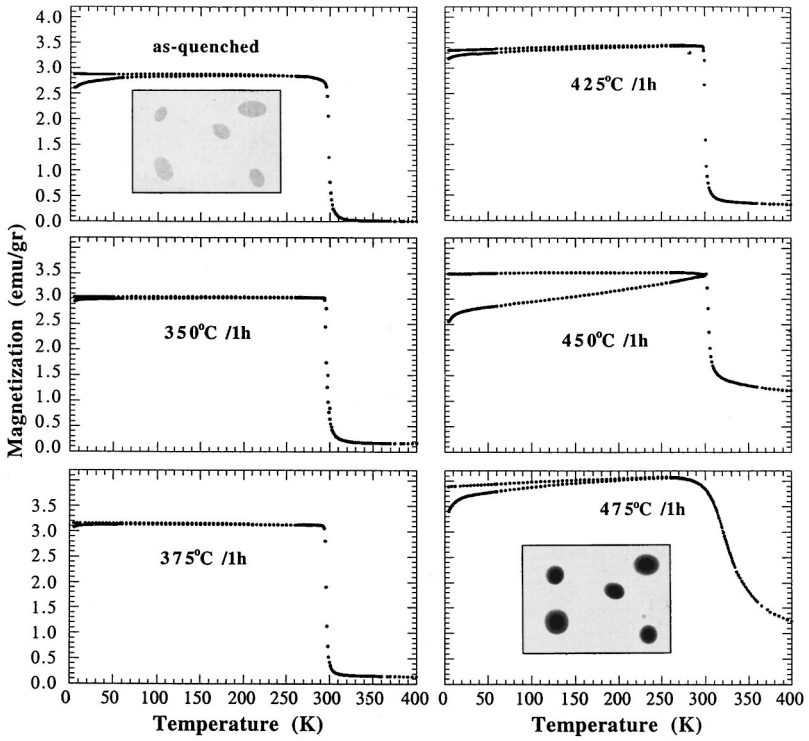

FIG. 2. Zero-field-cooling and field-cooling magnetization curves for all studied samples. Sketches showing an approximate view of the structural arrangement for the AQ and 475 °C sample conditions have been inserted in the plots. In the AQ condition, the inhomogeneities are amorphous clusters. In the sample heated at 475 °C 1 h, these inhomogeneities include a magnetic nanograin region, that is the nanometric crystallite+interface. Both inhomogeneities have been represented with the same shape in the sketches indicating the structural similarities presented between them. The different color intensities represent the different nature and density between the amorphous clusters and the nanograin regions.

inhomogeneities are of crystalline nature (α-Fe nanograins). It is important to remark here that the presented low-temperature magnetization data allow to characterize nanocrystal samples (ES) with a similar magnetic behavior as the AQ ones. Furthermore, the magnetization data for a sample annealed at higher temperatures show that the Curie temperatures of the amorphous phase are higher than the available temperatures in the SQUID apparatus. Besides, such a thermal treatment results in samples with much larger sizes and crystalline fraction (at least 23 nm and 40 at. %, respectively, deduced from x-ray diffraction and Mössbauer data[20]) and, so, these samples are not representative of the situation covered in the present discussion.

Given the similarities found in the AQ and ES conditions, it is useful to interpret quantitatively the data for the ES samples for an eventual extrapolation to the AQ state. For that, we can consider a recently reported model based on geometrical considerations and field penetration depth.[20] In the following, we will use this model to discuss the presented data.

The main parameters of the model are the size of the nanograins (D), the distance between them (d) and the atomic crystallized fraction (x). These parameters are summarized in first three columns in Table I. The grain size was derived from the x-ray-diffraction pattern using the Scherrer formula and the crystallized fractions were obtained from the fittings of the Mössbauer spectra. The crystallites are found to be nanometric, as it is typical of this composition and the size and the crystalline fraction increase when the annealing temperature is raised, as has been extensively reported.[4,28]

Finally, it is possible to estimate the average distance between crystals (d) assuming cubic or spherical crystals of the same size and disposed either in a simple cubic lattice or in a fcc arrangement as described elsewhere,[20,28]

$$d = D[Cx^{-1/3} - 1], \quad \text{with } 1 \geqslant C \geqslant (\sqrt{2}\pi/6)^{1/3},$$

depending on the arrangement. These estimations have been used successfully to explain, for example, the Curie temperature variations with the amount of the crystallized fraction.[20,33]

The ratios of the nanocrystalline magnetization to the total magnetization can be calculated using the values of the Fe magnetic moment in the amorphous ($\approx 1.5\mu_B$) (Ref. 19) and crystalline bcc phases ($2.2\mu_B$) and the crystalline fractions obtained from the Mössbauer spectra. These quantities appear in Table I as $M(X\text{tal})$ and can be compared to experimental $M(400\,\text{K})/M(5\,\text{K})$ ratio obtained by Arrot plots of the saturation magnetization data from the $M(H)$ curves. Figure 3 shows, as an example, the $M(H)$ curves of the sample annealed at 450 °C. The values of the experimental ratio are also inserted in Table I. The comparison to the former $M(X\text{tal})$ values shows a large discrepancy between them. The magnetization measured at 400 K is much larger than the expected one for the amount of nanocrystalline Fe. However, it is possible to include the contribution from the interface to the magnetization above T_C taking into account both: (i) the hyperfine field of this region, and (ii) the resonant area of its subspectrum (see Fig. 1). On the one hand from (i) and given that $Bhf = 30\,\text{T}$ in the interface, an ex-

TABLE I. Experimental and calculated data for the samples in all the analyzed conditions (see the text for details). Grain size (D), intergrain distance (d), crystalline fraction (%). Minimum and maximum values of the latter are given, depending on the shape and arrangement of the nanocrystals assumed in the model. $M(X\text{tal})$: magnetization of the crystal. $M(400\text{ K})/M(5\text{ K})$ (%): experimental ratio of the total magnetization. At. % interface: the interface amorphous-crystal percentage is deduced from the grain dimensions, assuming a ''thickness'' of two atomic layers, as deduced from the experimental value obtained for the sample treated at 475 °C 1 h, and higher temperatures.[20] $M(X\text{tal}+\text{interf})$: magnetization of the crystal+interface. Errors in brackets correspond to the last significative figure.

Treatment	Grain size D (nm)	Distance d (nm)	% crystal	$M(X\text{tal})$ calculated (%)	M (400 K)/M(5 K) (%)	At. % inter-face	M (Xtal+interf) calculated (%)
As-Q							
350 °C/1 h					5 (1)		
375 °C/1 h	≈5[a]	≈20[a]	1.0 (5)	2	5 (1)	1	3
425 °C/1 h	7 (2)	9–13	4 (1)	6	10 (1)	2	9
450 °C/1 h	8 (2)	8–12	5 (1)	9	13 (1)	3	12
475 °C/1 h	14 (1)	5–10	18 (2)	28	41 (2)	5	37

[a]Extrapolated from the higher temperature data. X-ray diffraction does not allow us to extract any value.

trapolated value for its Fe magnetic moments can be assumed about $2\mu_B$ (α-Fe values are $2.2\mu_B$ and $B_{\text{HF}}=33$ T). From (ii), the interface amount is obtained from fittings of the Mössbauer spectrum of the sample annealed at 475 °C and calculated in other samples assuming a constant thickness of 0.5 nm (≈2 atomic diameters). These are shown in the sixth column (at. % interface) in Table I. The product of the magnetic moment of the Fe atoms at the interface and the amount of Fe atoms provides the magnitude of the interface magnetization which is used to calculate the interface+grain magnetization [labeled as $M(X\text{tal}+\text{interf})$]. The last column in Table I displays the $M(X\text{tal}+\text{interf})$ values, which show a much better agreement with the experimental values $M(400\text{ K})/M(5\text{ K})$. This agreement shows the great importance of the interface in nanocrystalline materials and suggests that the magnetic nanograin region is formed by the nanometric crystallite plus the interface, strongly coupled to it.

Moreover, the sample annealed at 350 °C which neither showed any crystallinity in the Mössbauer spectra nor in the x-ray diffraction, presents a certain magnetization above T_C of the amorphous phase, which can be ascribed to magnetic

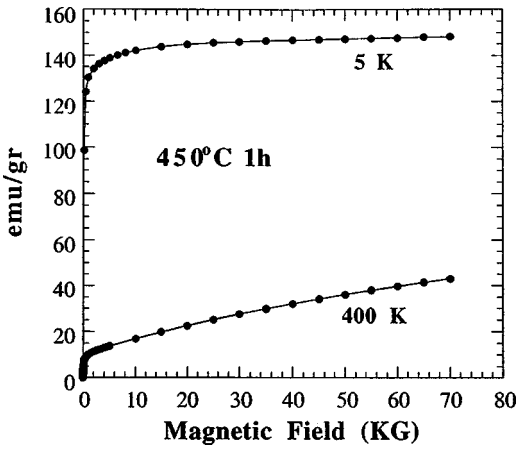

FIG. 3. First magnetization curves of the hysteresis loops of the sample annealed at 450 °C 1 h obtained at $T=5$ and 400 K.

entities. The nature of these latter is difficult to be precisely determined although they could be described as arising from a progressive nucleation of the nanocrystal seeds[16,34] and the growth of the very first nanograins. The fact that Mössbauer and x-ray diffraction are not able to detect them is not surprising; the first stages of the nanocrystallization probably produce highly disordered Fe aggregates around the Cu atoms which display broad diffraction peaks and a certain distribution of hyperfine fields. Consequently, they are masked by an otherwise predominant amorphous signal. However, ferromagnetic resonance (FMR) measurements performed on this sample shows the presence of a magnetic phase, different from the amorphous one, which carries high magnetization similar to that of the α-Fe.[29]

The inclusion of this interface into the magnetic grains slightly reduces the distance between them by about 1 nm, but this has also been taken into account in Table I. From the variation of the D and d values, it is clear that the first stages of crystallization produce very small grains separated by a distance which is large compared with their diameter. A crossover between grain size and intergrain distance occurs between the treatments at 450 and 475 °C close to the temperature range where the ZFC-FC splitting reaches to a maximum (see Fig. 2). At first glance, it seems that the factor affecting the freezing of the magnetic moments of the nanograins corresponds to the ratio of the distance to the diameter. We, however, feel that this is not the only parameter to be considered but also other mechanisms are playing, such as those that follow.

The splitting between the ZFC-FC curves is related to the difference between the random distribution of the nanograin moments and the fully ordered state which can be reached when cooling in a field. On the other hand, the degree of randomness in the ZFC state is determined by the coupling between the magnetic moments of the nanograins; in other words, the interaction between them. In a well-known physical picture,[35] a relevant parameter determining the coupling is the ratio of the distance between the nanoparticles (d) to the exchange-correlation length (L_{ex}) in the surrounding amorphous matrix expressed as

$$L_{ex} \approx (A/K_{eff})^{1/2}. \quad (1)$$

Here A is the exchange constant and K_{eff} an effective magnetic anisotropy, averaged in a volume of the order of L_{ex}^3.[21,22,36] If $L_{ex} > d$, the particles would remain coupled and no random blocking of the moments will take place. Alternatively, if $d \gg L_{ex}$, the Fe nanograins behave independently and a ''total'' random blocking can occur. There can be some long-range dipolar coupling correlating the behavior of the particles, but this is always feeble and will be still more in the actual case in which the amorphous matrix partially ''shields'' the magnetic moment of the grains.

The exchange coupling starts operating when the intergrain distance is about 10 nm. This is deduced from the progressive weakening of the splitting in the magnetization curves for samples 450/1 h and 475/1 h in Fig. 2. It can be argued that the exchange-correlation length in a soft ferromagnet[35] is about 35 nm and the grains should be coupled all the time and hence no splitting should be apparent. However, this is not observed for the case of samples at the early stages of crystallization. Hence the amount of magnetization assigned to the nanograins cannot be considered related directly to the magnitude of the ZFC-FC splitting of samples with low amounts of crystallization and, as mentioned earlier, coupling effects are an important factor. In this sense, some Fe grains decouple in the intermediate range, probably as the matrix starts to become inhomogeneous itself, and lose magnetic correlation, while for high crystallinity amounts the distance between grains decreases enough to still couple them. This latter regime can be obtained almost irrespective of the character of the amorphous matrix, as the distance between the grains is so low ($\approx$5 nm) that it allows the coupling through very hard magnets.

From the arguments just exposed regarding: (i) the magnitude of the magnetization above T_C in samples at the early stages of the crystallization, (ii) its explanation through a model dealing with magnetic nanograin regions, and (iii) the variation in the splitting of the low-temperature magnetization, it could be possible to anticipate the behavior of clusters in the as-quenched alloys. This is clearly indicated by the observed similarity between the magnetization shape of the curves for the as-quenched and annealed at 475 °C/1 h. This fact reveals the existence of a similar magnetic structure, of inhomogeneous nature (see sketches and caption in Fig. 2). Usual clusterlike models put forward for Fe-Zr seem to be backed up by this experimental finding. The difference comes here from the structure and size of the magnetic inhomogeneities: In the fully amorphous state, these inhomogeneities are regions of low-density amorphous arrangement[2,7] named ''spin clusters,'' whereas in the present case, those are small Fe nanograins plus their interface which are produced by annealing. This reinforces the attraction of the present annealings as a feasible route to produce case study samples. The similarity between nanocrystalline and as-quenched amorphous extends to the very low-temperature ($T < 50$ K) downturn of the magnetization in the ZFC curves. This may be attributed to a sudden increase of the magnetic anisotropy at low temperature, which further decouples the grains or clusters from the matrix. This anisotropy increase was responsible for the coercivity behavior in samples of similar composition as reported in Refs. 3 and 8.

In conclusion, we have shown that the presence of nanograins with high magnetization in a ferromagnetic matrix results in a large splitting of the ZFC and FC curves, when nanograins are magnetically decoupled. This behavior allows us to describe the as-quenched state of these samples as an inhomogeneous magnetic mixture of high magnetization clusters coupled through a lower magnetization matrix.

ACKNOWLEDGMENT

This work was supported by the Spanish CICYT under Grant No. MAT96/1023.

*Present address: Departamento de Física Aplicada II, Facultad de Ciencias, Universidad del País Vasco/EHU, Apartado 644, E-48080 Bilbao, Spain.

[1] H. Hiroyoshi and K. Fukamichi, J. Appl. Phys. **53**, 2226 (1982).
[2] S. N. Kaul, V. Siruguri, and G. Chandra, Phys. Rev. B **45**, 12 343 (1992).
[3] D. H. Ryan, J. M. D. Coey, E. Batalla, Z. Altounian, and J. O. Ström-Olsen, Phys. Rev. B **35**, 8630 (1987).
[4] K.. Fukamichi, T. Goto, H. Komatsu, and H. Wakabayashi, in *Physics of Magnetic Materials*, edited by W. Gorzkowski, H. K. Lachowicz, and H. Szymczak (World Scientific, Singapore, 1989), p. 354.
[5] S. N. Kaul, Phys. Rev. B **27**, 6923 (1983).
[6] H. Ren and D. H. Ryan, Phys. Rev. B **51**, 15 885 (1995).
[7] S. N. Kaul, J. Phys.: Condens. Matter **3**, 4027 (1991).
[8] D. Kaptas, T. Kemeny, L. F. Kiss, J. Balogh, L. Granasy, and I. Vincze, Phys. Rev. B **46**, 6600 (1992).
[9] L. F. Kiss, T. Kemeny, I. Vincze, and L. Granasy, J. Magn. Magn. Mater. **135**, 161 (1994).
[10] N. Hegman, L. F. Kiss, and T. Kemeny, J. Phys.: Condens. Matter **6**, L427 (1994).
[11] J. M. Barandiarán, P. Gorria, J. C. Gómez Sal, L. Fernández Barquín, and S. N. Kaul, IEEE Trans. Magn. **30**, 4776 (1994).
[12] J. M. Barandiarán, P. Gorria, I. Orue, M. L. Fdez-Gubieda, F. Plazaola, and A. Hernando, Phys. Rev. B **54**, 3026 (1996).
[13] M. L. Fdez-Gubieda, P. Gorria, J. M. Barandiarán, and L. Fernández Barquín, Nucl. Instrum. Methods Phys. Res. B **97**, 206 (1995).
[14] A. Makino, K. Suzuki, A. Inoue, Y. Hirotsu, and T. Masumoto, J. Magn. Magn. Mater. **133**, 329 (1994).
[15] K. Suzuki, A. Makino, A. Inoue, and T. Masumoto, J. Appl. Phys. **70**, 6232 (1991).
[16] N. Kataoka, A. Innoue, T. Masumoto, Y. Yoshizawa, and K. Yamauchi, Jpn. J. Appl. Phys., Part 2 **28**, L1820 (1989).
[17] G. Herzer, *Handbook of Ferromagnetic Materials*, edited by K. H. J. Buschow (Elsevier Science, Amsterdam, 1997), Vol. 10, p. 415.
[18] P. Allia, M. Baricco, P. Tiberto, and F. Vinai, in *Studies of Magnetic Properties of Fine Particles and their Relevance to Materials Science*, edited by J. L. Dormann and D. Fiorani (Elsevier Science Publishers, Amsterdam, 1992).
[19] J. M. Barandiarán, P. Gorria, I. Orúe, M. L. Fernández-Gubieda, F. Plazaola, J. C. Gómez Sal, L. Fernández Barquín, and L. Fournes, J. Phys.: Condens. Matter **9**, 5671 (1997).

[20] J. S. Garitaonandia, D. S. Schmool, and J. M. Barandiarán, Phys. Rev. B **58**, 12 147 (1998).
[21] J. Arcas, A. Hernando, J. M. Barandiarán, C. Prados, M. Vázquez, P. Marín, and A. Neuweiler, Phys. Rev. B **58**, 5193 (1998).
[22] A. Hernando, P. Marín, M. Vázquez, J. M. Barndiarán, and G. Herzer, Phys. Rev. B **58**, 366 (1998).
[23] A. Slawska-Waniewska and J. M. Grenèche, Phys. Rev. B **56**, R8491 (1997).
[24] T. Kemény, D. Kaptás, J. Balogh, L. F. Kiss, T. Pusztai, and I. Vince, J. Phys.: Condens. Matter **11**, 2841 (1999).
[25] N. Randrianantoandro, A. Slawska-Waniewska, and J. M. Greneéche, Phys. Rev. B **56**, 10 797 (1997).
[26] L. Fernández Barquín, F. Perrichon, and J. C. Gómez Sal, in *Nanostructured and Non-crystalline Materials*, edited by M. Vázquez and A. Hernando (World Scientific, Singapore, 1995), p. 557.
[27] D. Gómez Plaza, L. Fernández Barquín, J. García Soldevilla, R. Antras, and J. C. Gómez Sal, Solid State Commun. **102**, 353 (1997).
[28] J. S. Garitaonandia, Ph.D. thesis, Universidad del País Vasco, Bilbao, 1998.
[29] D. S. Schmool, J. S. Garitaonandia, and J. M. Barandiarán, Phys. Rev. B **58**, 12 159 (1998).
[30] R. A. Brand, J. Lauer, and D. Herlach, J. Phys. F: Met. Phys. **14**, 555 (1984).
[31] J. M. Greneche and A. Slawska-Waniewska, in *Non-crystalline and Nanoscale Materials*, Proceedings of Fifth International Workshop on Non-crystalline Solids, edited by R. Rivas and M. A. López-Quitela (World Scientific, Singapore, 1998), p. 233.
[32] M. Miglierini and J. M. Greneche, J. Phys.: Condens. Matter **9**, 2302 (1997); **9**, 2321 (1997).
[33] A. Hernando, I. Navarro, and P. Gorria, Phys. Rev. B **51**, 3281 (1995).
[34] K. Hono, K. Hiraga, Q. Wang, A. Inoue, and T. Sakurai, Acta Metall. Mater. **40**, 2137 (1992).
[35] G. Herzer, IEEE Trans. Magn. **25**, 3327 (1989).
[36] G. Herzer, IEEE Trans. Magn. **26**, 1397 (1990).